

# Influence of pH and Temperature on Basaluminite Dissolution Rates

Patricia Acero<sup>1</sup> and Karen A. Hudson-Edwards<sup>1,2\*</sup>

<sup>1</sup>Department of Earth and Planetary Sciences, Birkbeck, University of London, Malet St., London WC1E 7HX, UK.

<sup>2</sup> Now at Environment & Sustainability Institute and Camborne School of Mines, University of Exeter, Penryn, Cornwall, TR10 9FE, UK. \*Corresponding author Tel: +44-(0)1326-259-489; Email: [k.hudson-edwards@exeter.ac.uk](mailto:k.hudson-edwards@exeter.ac.uk)

Accepted by: *ACS Earth and Space Chemistry*

Date of acceptance: 16 January 2018

Keywords: basaluminite; aluminum; dissolution; rate; incongruent; activation energy.

TOC Art:



## Basaluminite Dissolution

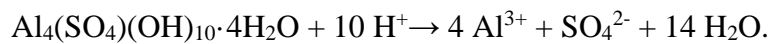
$$rate_{Al} = 10^{7.3 \pm 0.5} a_{H^+}^{0.64 \pm 0.04} e^{-78 \pm 3TRT}$$

## Abstract

The processes, rates, and controlling factors of basaluminite ( $\text{Al}_4(\text{SO}_4)(\text{OH})_{10}\cdot 4\text{H}_2\text{O}$ ) dissolution were assessed using batch dissolution experiments in both  $\text{H}_2\text{SO}_4$  and  $\text{HCl}$  at pHs of 2.4, 2.9-3.1, 3.5-3.6 and 4.0-4.1, and temperatures of c. 279, 293, 303 and 312 K. Basaluminite dissolution is incongruent over most of the studied pH range, giving generally a lower Al/S ratio in solution than in the pristine basaluminite sample. The lower Al/S ratio may be at least partially explained by the preferential release of sulfate compared to Al from the dissolving basaluminite. The dissolution rates range between  $10^{-7.6}$  and  $10^{-9.1}$   $\text{mol}\cdot\text{m}^{-2}\cdot\text{s}^{-1}$ . At 291-293K, the slowest rates were observed at pH 4.1 in  $\text{H}_2\text{SO}_4$  solutions, while at pH 3.0, the slowest rates were observed at 279 K in  $\text{HCl}$  solutions. Decreases in pH and increases in temperature increase dissolution rates. The influence of pH and temperature on the basaluminite dissolution rate, expressed as Al release, can be described by the following expression:

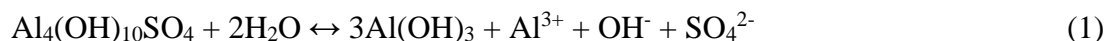
$$\text{rate}_{\text{Al}} = 10^{7.3\pm 0.5} a_{\text{H}^+}^{0.64\pm 0.04} e^{-78\pm 3/RT}$$

Where  $\text{rate}_{\text{Al}}$  is the basaluminite dissolution rate, based on the rate of Al release from dissolving basaluminite (in  $\text{mol}\cdot\text{m}^{-2}\cdot\text{s}^{-1}$ );  $a_{\text{H}^+}$  is the activity of hydrogen ions in solution;  $R$  is the Universal gas constant (in  $\text{kJ}\cdot\text{mol}^{-1}\cdot\text{K}^{-1}$ ) and  $T$  is temperature (in K). In light of the calculated value for the activation energy ( $78\pm 3$   $\text{kJ}\cdot\text{mol}^{-1}$ ), basaluminite dissolution appears to be surface-controlled. The reaction for basaluminite dissolution under the experimental conditions is proposed to be

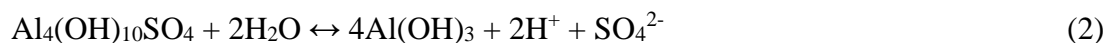


## INTRODUCTION

Basaluminite ( $\text{Al}_4(\text{SO}_4)(\text{OH})_{10} \cdot 4\text{H}_2\text{O}$ ) is one of the most common aluminum hydroxysulfates associated with acid mine drainage and acid sulfate soils<sup>1-5</sup> and is one of the main minerals thought to control the solubility of Al in acid sulfate waters<sup>1</sup>. Basaluminite is a nano-sized to microcrystalline variety of felsöbányaite<sup>6,7</sup> and was discredited by the International Mineralogical Association in 2006. However, we retain the term ‘basaluminite’ in this manuscript, as others have<sup>8</sup>, because of its prevalence in the scientific literature and in thermodynamic databases. There has been some controversy about the mechanisms and products of basaluminite dissolution<sup>1,2,9</sup>. Adams and Rawajfih<sup>1</sup> proposed that basaluminite dissolved incongruently, producing Al hydroxide as a secondary product:



Nordstrom<sup>3</sup> refuted this proposed equation because of the preferential formation of basaluminite from low pH waters, and because the aluminum ion cannot be independent of the solid phases present at chemical equilibrium<sup>9</sup>. Nordstrom<sup>3</sup> proposed the following alternative reaction for incongruent basaluminite dissolution:



Excessive concentrations of aluminum can lead to toxicity in plants<sup>10</sup>, animals<sup>11</sup>, particularly fish<sup>12</sup>, and humans<sup>11,13</sup>. To protect environmental health and to better predict the controls on Al cycling in the surface environment, there is a need to understand the mechanisms, rates and products of the dissolution of Al-bearing minerals such as basaluminite. Previous studies have determined the dissolution kinetics of the Al oxyhydroxysulfate alunite<sup>14,15</sup>, but those for basaluminite remain unknown. To help bridge this knowledge gap, the kinetics of basaluminite dissolution under conditions similar to those commonly found in low-temperature aquatic acid mine drainage

environments are assessed in this work. With this aim, batch dissolution experiments in both H<sub>2</sub>SO<sub>4</sub> and HCl at pH values between 2.5 and 4, at temperatures between 279 and 312 K were carried out using pure synthetic basaluminite as a starting material. The evolution of dissolved concentrations and reacting solids during the experiments were monitored and interpreted, together with geochemical modelling and mineralogical analyses. Rate expressions including the influence of pH and temperature were obtained, and possible dissolution reactions are discussed. Therefore, our study is the first to derive dissolution rate data for basaluminite that can be used to predict its environmental behavior.

## **MATERIALS AND METHODS**

**Analytical, mineralogical and other techniques.** Elemental analyses (for Al and S) for all solutions obtained in this study were obtained via Inductively Coupled Plasma Optical Emission Spectrometry (ICP-OES) on a Varian 720-ES (axial configuration) using a simultaneous solid-state detector (CCD). Calibration with sets of five standards was performed and laboratory standards were also analyzed after every 10 samples and any drift in the measurements (generally less than 4%) was corrected accordingly. The quantification limits for Al and S were determined to be  $3.7 \times 10^{-6}$  and  $3.1 \times 10^{-6}$  mol L<sup>-1</sup>, respectively. Sulfur concentrations were transformed to dissolved sulfate, which is the main stable species under the experimental conditions.

XRD spectra were acquired using a PANalytical XPert Pro diffractometer with Co K $\alpha_1$  radiation and an 'X'Celerator' position-sensitive detector with the X-ray tube operated at 40 kV and 30 mA. Data were collected over the 2 $\theta$  range from 5° to 110°, with a collection time of 13 h.

The surface area of the synthetic material was determined to be  $55.6 \pm 0.2 \text{ m}^2 \cdot \text{g}^{-1}$  using the BET method<sup>16</sup> in a Beckman Coulter SA3100 surface area analyzer using 5-point N<sub>2</sub> adsorption isotherms.

Variations of pH and temperature during the dissolution experiments were monitored by regular measurements using a Thermo Scientific Orion Star A121 pH meter with automated temperature correction. The pH meter was calibrated and checked using certified pH 2, 4 and 7 buffer solutions.

**Synthesis and characterisation of basaluminite.** Basaluminite was synthesized by titration using a modification of the method of Adams and Rawajfi<sup>1</sup>. For the synthesis, a 0.02 M Al<sub>2</sub>(SO<sub>4</sub>)<sub>3</sub> solution was titrated dropwise with 1 M NaOH while vigorously stirring to pH 4.2. The solution was decanted and filtered, thoroughly washed with deionized water and then filtered again and dried at room temperature for five days.

The purity of the obtained synthetic mineral phase was confirmed by XRD spectra, which showed a typical basaluminite diffraction pattern without any other peaks or significant background from other phases (Figure S1).

The composition of the synthetic precipitate was confirmed by ICP-OES after digestion with concentrated nitric acid. The formula of the resulting precipitate, based on the aluminum and sulfur proportions from the analyses, is Al<sub>3.98</sub>(SO<sub>4</sub>)(OH)<sub>10</sub>·nH<sub>2</sub>O. This corresponds to an almost perfectly stoichiometric basaluminite.

**Dissolution experiments.** The effect of different pH values and temperatures on basaluminite dissolution kinetics was assessed by means of batch stirred experiments in H<sub>2</sub>SO<sub>4</sub> solutions at pH values between 2.4 and 4.1 and at four different temperatures (around 279, 293, 303 and 312 K; see Table 1). This range of conditions is intended to represent the most usual conditions under

basaluminite dissolution may take place in natural systems. Although higher pH values were also explored in preliminary experiments, they led to oversaturated solutions with respect to basaluminite within a few minutes and, therefore, they have not been included in this study. The experiments at the two lowest temperatures were carried out in a controlled temperature room and the rest were performed using a magnetic stirred heating plate. The effect of HCl solutions on the dissolution kinetics was also explored between 293 K and 295 K and under the same pH range (2.4 to 4.0) as for the H<sub>2</sub>SO<sub>4</sub> experiments. All the reported conditions were addressed at least by triplicate (and in most cases by quadruplicate) experiments to ensure the reproducibility of the obtained results.

For each dissolution experiment, approximately 50 mg was quartered and split from of the synthetic basaluminite sample and placed in a beaker containing 200 mL of the target solution. All the solutions were prepared using deionized water ( $<18 \text{ M}\Omega \cdot \text{cm}^{-1}$ ) by adding the required amounts of concentrated ultrapure H<sub>2</sub>SO<sub>4</sub> or HCl to reach the target pH. The mixture was stirred by a pivoting stirring bar at 400 rpm at the desired temperature; this stirring procedure produced a homogeneous sample suspension while minimizing grinding during the experiments.

The pH value was regularly monitored throughout the experiments and corrected to avoid drifting (i.e. pH deviations from the initial value larger than 0.1 pH units). This was only observed, as a pH increase, in some of the experiments at pH above 3. For those cases, pH drifting was avoided by dropwise adding ultrapure HCl 1M.

During the dissolution experiments, 4 mL aliquots of the reacting suspension were sampled every 3 to 50 minutes (depending on the dissolution rates under different pH and temperature conditions, as determined in preliminary experiments), filtered through disposable syringe filters with a pore size below 0.2  $\mu\text{m}$  and immediately acidified with ultrapure concentrated HNO<sub>3</sub>, before

storing them refrigerated for analysis of Al and S concentrations by ICP-OES. Some of the experimental conditions explored in this study required less than one hour of dissolution, while several hours of interaction were necessary in other cases to obtain the reported rates.

For the calculation of the dissolution rates, Al and sulfate concentrations were corrected by subtracting their values in the first suspension aliquot, sampled after 2 to 5 minutes of solid-solution interaction. This procedure, already used in earlier studies<sup>14,17</sup>, allows the sulfate concentrations in most of the experiments carried out in H<sub>2</sub>SO<sub>4</sub> solutions to be estimated. However, the uncorrected concentrations were retained for the speciation calculations.

Speciation calculations were carried out using the PHREEQC code<sup>18</sup> and the wateq4f.dat<sup>19</sup> thermodynamic database distributed with the code.

**Dissolution rates and rate equations.** Dissolution rates were obtained from the slope of the linear fitting of concentrations vs time for each dissolution experiment and normalized with respect to the initial surface area of the synthetic basaluminite. After discarding any clear outliers, the experimental dissolution rates were fitted as a function of pH and temperature by multiple linear regression. The significance of the fitted parameters was verified by using t-tests and the fitting residuals were examined to ensure the absence of statistical outliers in the dataset.

## RESULTS AND DISCUSSION

**Evolution of Al and S dissolved concentrations throughout the dissolution experiments, and possible dissolution mechanisms.** The main results obtained in the dissolution experiments are displayed in Table 1. During the experiments, aluminum concentrations evolved linearly with time, which allowed us to obtain the rates of Al release from dissolving basaluminite. A similar trend was also observed for estimated sulfate contents in most of the experiments but

with a weaker linear correlation of sulfate concentrations versus time of experiment. Thus, the evolution of sulfate concentrations was only used to determine dissolution rates in the experiments with HCl. Moreover, the concentrations at the end of all the experiments were used to estimate the approximate Al/S molar ratios due to basaluminite dissolution. The amount of basaluminite dissolved during the experiments can be estimated from Al concentrations and using the initial stoichiometry of the synthetic mineral. This dissolved weight represents less than 10% of the initial solid in all the experiments except for that at pH 3 and 312 K, for which a loss of around 30% of the initial sample is estimated.

As displayed in Table 1 and Figure 1, the obtained Al release rates from dissolving basaluminite range between  $10^{-7.6}$  and  $10^{-9.1}$  mol·m<sup>-2</sup>·s<sup>-1</sup>, with the lowest values corresponding to the experiments with H<sub>2</sub>SO<sub>4</sub> at 292 K and pH 4.1, and the highest to the experiments H<sub>2</sub>SO<sub>4</sub> at 312 K and pH 3.1. Dissolution rates for the H<sub>2</sub>SO<sub>4</sub> experiments are higher than those for the HCl experiments (Table 1). This agrees with other dissolution studies involving Al phases, especially gibbsite. For example, dissolution experiments carried out for gibbsite in different anionic environments at pH 3.5 by Mogollón et al.<sup>20</sup> showed that dissolution rates in sulfate solutions are almost five times faster than in chloride solutions under otherwise identical conditions. Ridley et al.<sup>21</sup> demonstrated that the dissolution rate of gibbsite in sulfate solutions is approximately 10 times faster than in chloride solutions for experiments under constant pH and ionic strength, and a similar trend was noted by Dietzel and Böhme<sup>22</sup>. According to Mogollón et al.<sup>20</sup>, a possible explanation for this observation is the fact that monovalent anions such as Cl<sup>-</sup> may interact with the surface mainly as electrostatic outer-sphere complexes, whereas SO<sub>4</sub><sup>2-</sup> could act as a catalyst due to an inner-sphere interaction that could weaken Al-OH bonds at the gibbsite surface and thus increase dissolution



rates. A similar interaction between aqueous  $\text{SO}_4^{2-}$  and Al-OH bonds in the basaluminite Al octahedra (see below for discussion of basaluminite structure) could be operating in our dissolution experiments.

Basaluminite dissolution seems to be an incongruent process under most of the target experimental conditions. As shown in Table 1 and Figure 2, the dissolved Al/S molar ratios are generally below 3.5, being therefore lower than the same ratio in the initial synthetic basaluminite (i.e., ratio of 4). This ratio is low for the HCl experiments (mostly below 4), particularly low (below 3) for most of the experiments using  $\text{H}_2\text{SO}_4$  solutions and it is even below 2 for the experiments at pH 4 using both  $\text{H}_2\text{SO}_4$  and HCl solutions (Table 1; Figure 2). These observations imply that either that sulfate is being preferentially released to solution over aluminum or that aluminum is precipitating from the target solutions.

To further evaluate the reason for the low Al/S molar ratios, speciation calculations were carried out with the PHREEQC code for the experimental solutions. The results show that, amongst the different aluminum phases present in the wateq4f.dat database, thermodynamic equilibrium is only reached with respect to diasporite ( $\text{AlO}(\text{OH})$ ) and only for the experiments at pH at 4.1 and 293K (Table S1). In light of these results, secondary precipitation of Al-bearing phases does not seem to be the general cause for the low dissolved Al/S molar ratios observed in the reacting solutions. Thus, a possible explanation for the observed incongruent dissolution in those cases would be the preferential release of  $\text{SO}_4$  relative to Al during basaluminite dissolution. Even for the experiments at pH 4, the hypothesis of diasporite precipitation does not fully explain the observed results. As displayed in Table 1 and Figure 2, even though both HCl and  $\text{H}_2\text{SO}_4$  experimental solutions at pH around 4 are similarly close to equilibrium with respect to diasporite, dis-

solved Al/S molar ratios are much lower for the H<sub>2</sub>SO<sub>4</sub> solutions. Thus, the hypothesis of a preferential release of sulfate over aluminum from the dissolving basaluminite seems to be more consistent with the observed dissolved molar Al/S ratios during the experiments.

This behavior may be related to the structure of basaluminite, which is based on stacked octahedral sheet of aluminum hydroxide formed by zigzag ribbons extending along [010] that bond together to form Al<sub>8</sub>O<sub>22</sub> layers<sup>6</sup>. Isolated sulfate tetrahedra and H<sub>2</sub>O groups occur in the interlayer between these sheets, and they are bonded to each other and to the sheets by H-bonding<sup>6,23</sup>. The preferential release of sulfate from dissolving basaluminite seems consistent with its interlayer structural position, which is more weakly bound within the mineral than the octahedrally-coordinated Al atoms. Preferential release of sulfate during dissolution of other oxyhydroxysulfates, including jarosite<sup>24</sup>, has also been observed and attributed to similar structural features.

In the H<sub>2</sub>SO<sub>4</sub> dissolution experiments at c. 292K, the dissolved Al/S molar ratio is low at pH 4.0 (0.7-0.9), and increases with decreasing pH (pH 3.6: 0.5-2.1; pH 2.9: 1.7-3.0; Table 1; Figure 2). This may be related to the increasing positive charge of basaluminite surfaces due to protonation with the pH decrease. Although no published data about the pH of potential of zero charge (PZC) for basaluminite have been found, this value has been reported to be between 6 and 9 in other aluminum oxides and hydroxides<sup>25,26</sup>. If similar values are assumed for basaluminite, this would imply the existence of positively charged surfaces under the whole range of conditions explored in this work, with the positive net charge increasing with the pH decrease. The increase of surface positive charge is expected to enhance the retention of sulfate groups linked to the surface, which would be consistent with the higher dissolved Al/S molar ratios with increasing acidity. A similar trend has been proposed in earlier studies for other types of minerals (e.g. goethite<sup>27</sup>) and for variable surface charged soils<sup>28-30</sup>. Although the adsorption mechanisms of sulfate ions to

aluminum phases under low pH conditions are not completely understood, both electrostatic attraction on positive sites and inner-sphere complexation via a ligand exchange mechanism<sup>31,32</sup> seem to be possible.

The trend of increasing dissolved Al/S molar ratio with decreasing pH in the experiments with H<sub>2</sub>SO<sub>4</sub> at 292K does not continue with the pH 2.4 experiments, when the ratio decreases to 0.6-1.0 (Table 1; Figure 2). Unfortunately, we cannot offer a fully-supported explanation for this observation with the currently available data. We hypothesize that this may be related to the change in sulfur aqueous speciation and with the increasing activity of bisulfate (HSO<sub>4</sub><sup>-</sup>) at low pH<sup>33</sup>. In this case, a fraction of the available hydrogen ions would bond with sulfate to form bisulfate. This may reduce the protonation of the basaluminite surface and contribute to increase the release of sulfate ions from the basaluminite structure. . Some of the aqueous sulfate would also form AlSO<sub>4</sub><sup>+</sup> aqueous complexes, which dominate the Al speciation under these experimental conditions (Table 2). In any case, the question of the non-linear evolution of Al/S dissolved ratios for the basaluminite dissolution experiments with H<sub>2</sub>SO<sub>4</sub> remains open.

Overall, the molar Al/S ratios are lower for the experiments with H<sub>2</sub>SO<sub>4</sub> solutions compared to those with HCl solutions (Table 1; Figure 2). We hypothesize that this is related to the weakening of the Al-OH bonds by SO<sub>4</sub><sup>2-</sup> which would destabilize the basaluminite structure<sup>20</sup>. This would allow dissolution to proceed by both release of Al and preferential release of SO<sub>4</sub> (as described above). This would occur to a greater degree than in the HCl experiments where there would be no weakening of the Al-OH bonds by sulfate. Thus, although it would at first appear that such destabilization of the Al-OH bonds in the H<sub>2</sub>SO<sub>4</sub> experiments would lead to increased release of Al to solution, this is not recorded due to the preferential release of sulfate from the dissolving basaluminite.

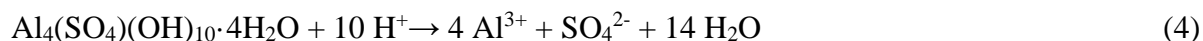
**Basaluminite dissolution rates.** The data in Table 1 and Figure 1 indicate that Al release rates from dissolving basaluminite increase in a linear fashion with decreases in pH and increases in temperature (Figure 1; Table 1). The rate expression obtained by multiple linear regression of the experimental rates is:

$$rate_{Al} = 10^{7.3 \pm 0.5} a_{H^+}^{0.64 \pm 0.04} e^{-78 \pm 3/RT} \quad (3)$$

where  $rate_{Al}$  is the Al release rate from dissolving basaluminite (in  $\text{mol} \cdot \text{m}^{-2} \cdot \text{s}^{-1}$ );  $a_{H^+}$  is the activity of hydrogen ions in solution;  $R$  is the Universal gas constant (in  $\text{kJ} \cdot \text{mol}^{-1} \cdot \text{K}^{-1}$ ) and  $T$  is temperature (in K). As shown in Eq. 3, the value of the activation energy, which represents the dependence of basaluminite dissolution rate on temperature, is approximately  $78 \pm 3 \text{ kJ} \cdot \text{mol}^{-1}$  for pH values between 2.5 and 4.1. This energy value is similar to that proposed by Elwood-Madden et al.<sup>34</sup> for jarosite dissolution ( $79 \text{ kJ} \cdot \text{mol}^{-1}$ ), and higher than the values usually considered to correspond to diffusion-controlled dissolution kinetic mechanisms (less than around  $20 \text{ kJ} \cdot \text{mol}^{-1}$ <sup>35,36</sup>). Thus, basaluminite dissolution kinetics seem to be surface-controlled in light of the obtained activation energy value.

Alunite dissolution rates between  $10^{-10}$  and  $10^{-11} \text{ mol} \cdot \text{m}^{-2} \cdot \text{s}^{-1}$ <sup>14,15</sup> are more than one order of magnitude slower than basaluminite dissolution rates under similar conditions. This is consistent with the much lower crystallinity of basaluminite (cf., the broad diffraction peaks in Figure S1), and confirms field and laboratory observations of the metastability of basaluminite and the fact it recrystallizes into phases such as alunite and gibbsite<sup>2,3,37</sup>. Alunite dissolution rates also increase with decreases in pH and increases in temperature but the dependence is much weaker than for basaluminite<sup>14</sup>. Like alunite dissolution below pH 4.8<sup>14</sup>, there is increasing formation of  $\text{Al-SO}_4^+$  complexes with decreasing pH in the basaluminite experiments with  $\text{H}_2\text{SO}_4$  (Table 2).

**Overall dissolution reaction.** Basaluminite dissolution is generally incongruent at the pH conditions described by this study (pH 2.4 to 4.1). According to solubility calculations (Table S1), basaluminite dissolution under these conditions does not seem to lead to the precipitation of any secondary product. Thus, a plausible overall reaction expressing basaluminite dissolution under the conditions explored in this study could simply be:



This reaction would lead to the consumption of 10 mol of  $\text{H}^+$  for each mole of dissolved basaluminite. Therefore, basaluminite dissolution under unbuffered conditions within this pH range could lead to a pH increase. It was not possible to observe this in our experiments because pH drift was avoided by dropwise addition of HCl. The reverse of reaction 4 would involve the production of 10 moles of  $\text{H}^+$  for each mole of basaluminite precipitated, leading to a pH decrease. As previously reported by Sánchez-España et al.<sup>8</sup>, this would represent an important buffering mechanism during natural neutralization in AMD systems and during titration experiments.

The dissolution equation described by Eq. 4 differs from those of Adams and Rawajfi<sup>1</sup> and Nordstrom<sup>3</sup> (Eqs. 1 and 2, respectively), largely because of our observed pH dependence for basaluminite dissolution. The lack of a solid product in this equation and in our experiments can be explained by the fact that Al hydrolyses only above the pH range of our experiments (c. pH 4.5<sup>5,38,39</sup>), when the dissolved Al species changes from  $\text{Al}^{3+}$  to  $\text{Al}(\text{OH})_2^+$ <sup>5,40</sup>.

## SUPPORTING INFORMATION

The XRD pattern of the initial synthetic basaluminite sample, and the table of calculated saturation index values for main possible aluminum secondary phases. This material is available free of charge via the Internet at <http://pubs.acs.org>

## ACKNOWLEDGEMENTS

We acknowledge funding for this study provided by the EC Marie Curie Intra-European Fellowship program (Project entitled ‘Reactivity of Aluminum Sulfate Minerals in Mine Wastes’; RASMIM) through a fellowship to P.A. We thank Gareth Tarbuck (UCL, London, UK) for help with the geochemical analyses and mineralogical determinations and their interpretation. We also thank the reviewers whose comments significantly improved the manuscript.

## REFERENCES

- (1) Adams, F.; Rawajfih, Z. Basaluminite and alunite: a possible cause of sulfate retention by acid soils. *Soil Sci. Soc. Am. J.* **1977**, *41* (4), 686-692.
- (2) Prietzel, J.; Hirsch, C. Extractability and dissolution kinetics of pure and soil-added synthesized aluminum hydroxyl sulphate minerals. *Eur. J. Soil Sci.* **1998**, *49* (4), 669-681.
- (3) Nordstrom, D. K. The effect of sulfate on aluminum concentrations in natural waters: some stability relations in the system  $\text{Al}_2\text{O}_3\text{-SO}_3\text{-H}_2\text{O}$  at 298K. *Geochim. Cosmochim. Acta* **1982**, *46* (4), 681-692.
- (4) Nordstrom, D. K.; Ball, J. W.; Roberson, C. E.; Hanshaw, B. B. The effect of sulfate on aluminum concentrations in natural waters. II: Field occurrences and the identification of aluminum hydroxysulfate precipitates. *Proc. Geol. Soc. Am. Ann. Meeting* **1984**, pp. 611-621.

- (5) Bigham, J. M.; Nordstrom, D. K. Iron and aluminum hydroxysulfates from acid sulfate waters. In *Sulfate Minerals: Crystallography, Geochemistry, and Environmental Significance*; Alpers, C. N., Jambor, J., L., Nordstrom, S. K., Eds.; Mineralogical Society of America **2000**; pp. 351-403.
- (6) Farkas, L.; Pertlik, F. Crystal structure determinations of felsöbányaite and basaluminite,  $\text{Al}_4(\text{SO}_4)(\text{OH})_{10}\cdot 4\text{H}_2\text{O}$ . *Acta Mineral. Petrog. Szeged.* **1997**, *38*, 5-15.
- (7) Jambor, J. L.; Grew, E. S.; Roberts, A. C. New mineral names. *Am. Mineral.* **1998**, *83*, 1347-1352.
- (8) Sánchez-España, J.; Yusta, I.; Diez-Ercilla, M. Schwertmannite and hydrobasaluminite: A re-evaluation of their solubility and control on the iron and aluminium concentration in acidic pit lakes. *Appl. Geochem.* **2011**, *26*, 1752-1774.
- (9) Jones, A. M.; Collins, R. N.; Waite, T. D. Mineral species control of aluminum solubility in sulfate-rich acidic waters. *Geochim. Cosmochim. Acta* **2011**, *75* (4), 965-977.
- (10) Poschenrieder, C.; Gunsé, B.; Corrales, I.; Barceló, J. A glance into aluminum toxicity and resistance in plants. *Sci. Total Environ.* **2008**, *400*, 356-368.
- (11) Shaw, C. A.; Tomljenovic, L. Aluminum in the central nervous system (CNS): toxicity in humans and animals, vaccine adjuvants, and autoimmunity. *Immunol. Res.* **2013**, *56*, 304-316.
- (12) Muniz, I. P.; Leivestad, H. Acidification-effects on freshwater fish. In *Ecological Impact of Acid Precipitation*; Drabløs, D. A.; Tollan, A., Eds.; SNSF Proceedings, Oslo, **1980**, pp. 84-92.
- (13) Exley, C. The toxicity of aluminium in humans. *Morphologie* **2016**, *100*, 51-55.

- (14) Acero, P.; Hudson-Edwards, K. A.; Gale, J. D. Influence of pH and temperature on alunite dissolution: rates, products and insights on mechanisms from atomistic simulation. *Chem. Geol.* **2015**, *419*, 1-9.
- (15) Miller, J. L.; Elwood Madden, A. S.; Philips-Lander, C. M.; Pritchett, B. N.; Elwood Madden, M. E. Alunite dissolution rates: Dissolution mechanisms and implications for Mars. *Geochim. Cosmochim. Acta* **2016**, *172*, 93-106.
- (16) Brunauer, S.; Emmett, P. H.; Teller, E. Adsorption of gases in multimolecular layers. *J. Am. Chem. Soc.* **1938**, *60* (2), 309-319.
- (17) Welch, S. A.; Kirste, D.; Christy, A. G.; Beavis, F.R.; Beavis, S. G. Jarosite dissolution II – Reaction kinetics, stoichiometry and acid flux. *Chem. Geol.* **2008**, *254*, 73-86.
- (18) Parkhurst, D. L.; Appelo, C. A. J. Description of input and examples for PHREEQC version 3: a computer program for speciation, batch-reaction, one-dimensional transport, and inverse geochemical calculations. US Geological Survey Techniques and Methods, **2013**, book 6, chap. A43, 497 p.
- (19) Ball, J. W.; Nordstrom, D. K. User's manual for WATEQ4F, with revised thermodynamic database and test cases for calculating speciation of major, trace, and redox elements in natural waters. *U.S. Geol. Surv. Open-File Rep.* **1991**, *91-183*, 189.
- (20) Mogollón, J. L.; Pérez-Díaz, A.; Lo Monaco, S. The effects of ion identity and ionic strength on the dissolution rate of a gibbsitic bauxite. *Geochim. Cosmochim. Acta* **2000**, *64* (5), 781-795.
- (21) Ridley, M. K.; Wesolowski, D. J.; Palmer, D. A.; Bénézech, P.; Kettler, R. M. Effect of sulfate on the release rate of Al<sup>3+</sup> from gibbsite in low-temperature acidic waters. *Environ. Sci. Technol.* **1997**, *31* (7), 1922-1925.



- (22) Dietzel, M.; Böhme, G. The dissolution rates of gibbsite in the presence of chloride, nitrate, silica, sulfate, and citrate in open and closed systems at 20°C. *Geochim. Cosmochim. Acta* **2005**, *69* (5), 1199-1211.
- (23) Hawthorne, F. C.; Krivovichev, S. V.; Burns, P. C. The crystal chemistry of sulfate minerals. In *Sulfate Minerals: Crystallography, Geochemistry, and Environmental Significance*; Alpers, C. N., Jambor, J., L., Nordstrom, S. K., Eds.; Mineralogical Society of America **2000**; pp. 1-112.
- (24) Smith, A. M. L.; Hudson-Edwards, K. A.; Dubbin, W. E.; Wright, K. Dissolution of jarosite [KFe<sub>3</sub>(SO<sub>4</sub>)<sub>2</sub>(OH)<sub>6</sub>] at pH 2 and 8: insights from batch experiments and computational modeling. *Geochim. Cosmochim. Acta* **2006**, *70* (3), 608-621.
- (25) Wood, R.; Fornasiero, D.; Ralston, J. Electrochemistry of the boehmite—water interface. *Colloid Surface* **1990**, *51*, 389-403.
- (26) Kolics, A.; Polkinghorne, J. C.; Wieckowski, A. Adsorption of sulfate and chloride ions on aluminum. *Electrochim. Acta* **1998**, *43* (18), 2605-2618.
- (27) Zhang, P. C.; Sparks, D. L. Kinetics and mechanisms of sulfate adsorption / desorption on goethite using pressure-jump relaxation. *Soil Sci. Soc. Am. J.* **1990**, *54* (5), 1266-1273.
- (28) Gillman, G. P. The chemical properties of acid soils with emphasis on soils of the humid tropics. In: *Plant-soil Interactions at Low pH*. Eds. Wright, R. J., Baligar, V. C. R. P., Murrmann, R. P., Eds; Kluwer Academic Publishers, Dordrecht **1991**; pp 3-14.
- (29) Zhang, G. Y.; Brümmer, G. M.; Zhang, X. N. Effect of perchlorate, nitrate, chloride and pH on sulfate adsorption by variable-charge soils. *Geoderma* **1996**, *73* (3-4), 217-229.
- (30) Jung, K.; Ok, Y. S.; Chang, S. X. Sulfate adsorption properties of acid-sensitive soils in the Athabasca oil sands region in Alberta, Canada. *Chemosphere* **2011**, *84* (4), 457-463.

- (31) Violante, A.; Pigna, M.; Liu, F.; Huang, P. M.; Bollag, J. M.; Vityakon, P. Sorption/desorption of sulfate on/from variable charge minerals and soils: competitive effects of organic and inorganic ligands. In *Symposium 47 Soil Mineral-Organic Component-Microorganism Interactions and the Impact on the Ecosystem and Human Welfare* and *Symposium 06 Frontiers of Soil Chemistry and Biochemistry of the Soil Rhizosphere*; 17th World Congress of Soil Science, Bangkok, Thailand, 14-21 August 2002, Science Publishers, Inc. **2005**; pp. 195-221.
- (34) Elwood Madden, M.; Madden, A. S.; Rimstidt, J. D.; Zahrai, S.; Kendall, M. R.; Miller, M. A. Jarosite dissolution rates and nanoscale mineralogy. *Geochim. Cosmochim. Acta* **2012**, *91*, 306-321.
- (35) Lasaga, A. C. Rate laws of chemical reactions. In *Kinetics of Geochemical Processes*; Lasaga, A. C., Kirkpatrick, R. J., Eds.; Reviews in Mineralogy 8. Mineralogical Society of America, **1981**, pp. 1-68.
- (36) Lasaga, A. C. *Reaction Kinetics in Geosciences*. Princeton University Press, Princeton, New Jersey, **1998**.
- (37) Sánchez-España, J.; Yusta, I.; Burgos, W. D. Geochemistry of dissolved aluminum at low pH 4: Hydrobasaluminite formation and interaction with trace metals, silica and microbial cells under anoxic conditions. *Chem. Geol.* **2016**, *441*, 124-137.
- (38) Lukewille, A.; van Breemen, N. Aluminium precipitates from groundwater of an aquifer affected by acid atmospheric deposition in the Senne, Northern Germany. *Water Air Soil Poll.* **1992**, *63*, 411-416.
- (39) Sherriff, B. L.; Sidenko, N. V.; Salzsauler, K. A. Differential settling and geochemical evolution of tailings' surface water at the Central Manitoba Gold Mine. *Appl. Geochem.* **2007**, *22*, 342-356.

(40) Martell, A. E.; Motekaitis, R. J. Coordination chemistry and speciation of Al(III) in aqueous solution. *194th Annual Meeting of the American Chemical Society*, New Orleans, **1987**.

**Table 1.** Summary of results from dissolution experiments. Stdev log rate corresponds to the standard deviation of the set of replicate experiments carried out for each set of studied conditions.

pH	Solution type	T (K)	Approximated molar Al/S ratio <sup>1</sup>	Log rate Al (mol/m <sup>2</sup> .s)	Log rate SO <sub>4</sub> (mol/m <sup>2</sup> .s)	Stdev log rate Al	Stdev log rate SO <sub>4</sub>
3.0	H <sub>2</sub> SO <sub>4</sub>	279	n/a	-9.06	n/a	0.05	n/a
3.1	H <sub>2</sub> SO <sub>4</sub>	293	1.7-3.0	-8.65	n/a	0.04	n/a
3.0	H <sub>2</sub> SO <sub>4</sub>	303	2.3-4.1	-8.03	n/a	0.04	n/a
3.1	H <sub>2</sub> SO <sub>4</sub>	312	2.4-4.6	-7.62	n/a	0.07	n/a
2.4	H <sub>2</sub> SO <sub>4</sub>	291	0.6-1.0	-8.12	n/a	0.02	n/a
3.5	H <sub>2</sub> SO <sub>4</sub>	292	0.5-2.1	-8.92	n/a	0.06	n/a
4.1	H <sub>2</sub> SO <sub>4</sub>	292	0.7-0.9	-9.09	n/a	0.02	n/a
3.6	HCl	294	2.3-3.2	-8.94	-9.38	0.10	0.07
4.0	HCl	293	1.6-2.3	-8.94	-9.21	0.05	0.05
2.9	HCl	295	3.3-4.5	-8.86	-9.45	0.02	0.05
2.4	HCl	294	3.3-4.0	-8.70	-9.30	0.03	0.02

<sup>1</sup> Estimated at the end of the experiments.

**Table 2.** Distribution of Al dissolved species (in %) under the different conditions assessed in this study, as obtained from PHREEQC speciation calculations using the wateq4f.dat thermodynamic database. Species representing less than 1% of total Al are not displayed.

pH	Solution type	Al (mMol·L <sup>-1</sup> )	Sulfate (mMol·L <sup>-1</sup> )	T (K)	Al <sup>3+</sup> (%)	AlSO <sub>4</sub> <sup>+</sup> (%)	Al(OH) <sub>2</sub> <sup>+</sup> (%)	Al(SO <sub>4</sub> ) <sub>2</sub> <sup>-</sup> (%)
3.0	H <sub>2</sub> SO <sub>4</sub>	0.111	0.437	279	56.3	43.2	0.2	0.4
3.1	H <sub>2</sub> SO <sub>4</sub>	0.093	0.468	293	50.2	48.9	0.3	0.5
3.0	H <sub>2</sub> SO <sub>4</sub>	0.241	0.531	303	47.5	51.3	0.7	0.5
3.1	H <sub>2</sub> SO <sub>4</sub>	0.853	0.781	312	46.2	52.1	1.2	0.5
2.4	H <sub>2</sub> SO <sub>4</sub>	0.222	2.062	291	23.2	74.2	0.0	2.5
3.5	H <sub>2</sub> SO <sub>4</sub>	0.056	0.156	292	72.2	26.2	1.5	0.1
4.1	H <sub>2</sub> SO <sub>4</sub>	0.030	0.047	292	83.7	9.9	6.1	0.0
3.6	HCl	0.048	0.023	294	72.2	26.2	1.5	0.1
4.0	HCl	0.048	0.031	293	86.8	6.7	6.2	0.0
2.9	HCl	0.111	0.031	295	93.7	5.7	0.6	0.0
2.4	HCl	0.067	0.022	294	96.3	3.5	0.2	0.0

**Figure 1.** Basaluminite dissolution rates (in logarithmic scales) obtained in this study vs. pH and for different temperatures (a) and vs 1000/RT for the pH 3 experiments with H<sub>2</sub>SO<sub>4</sub> (b).

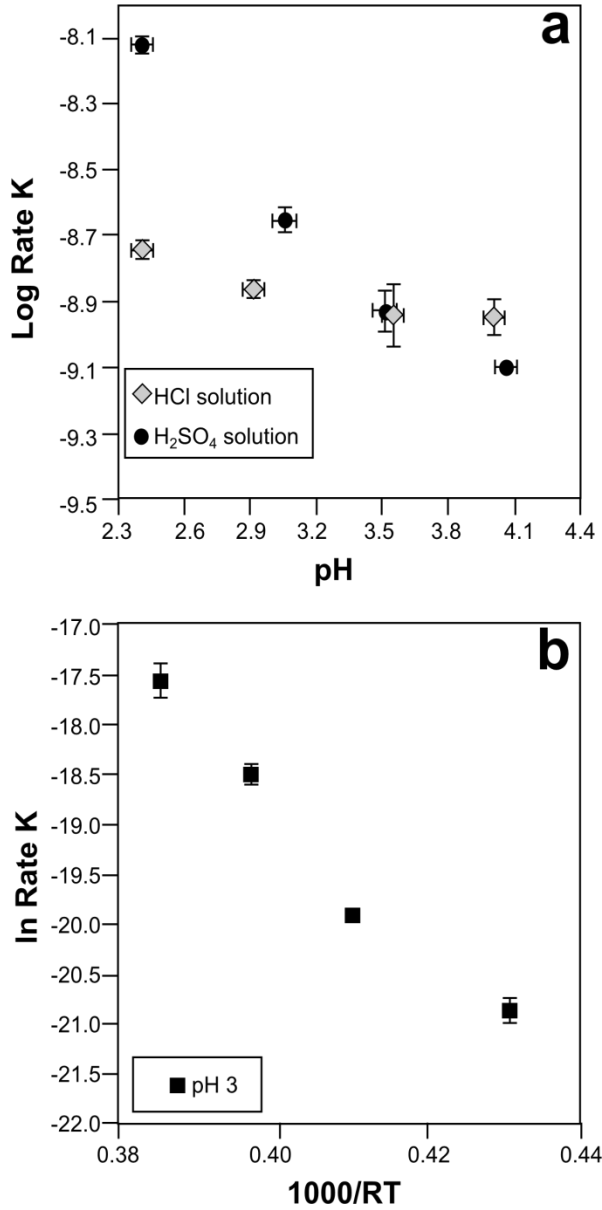
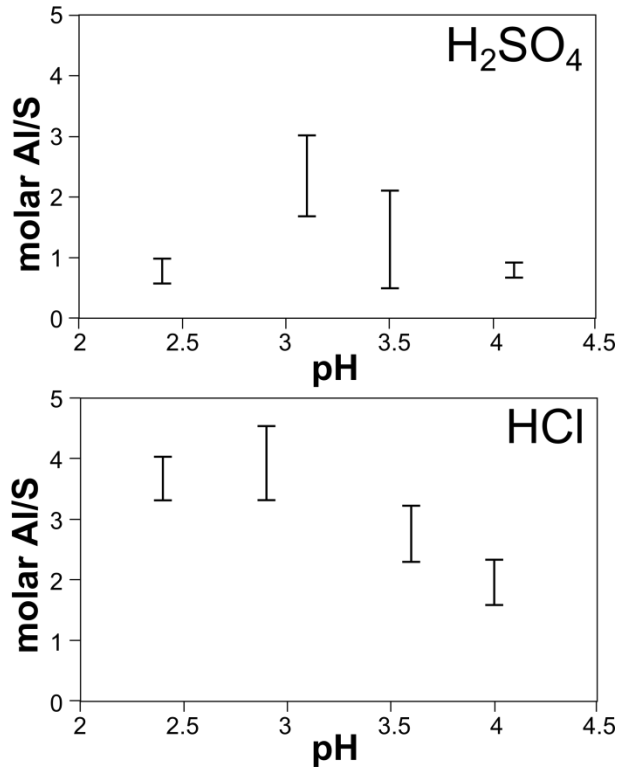


**Figure 2.** Ranges of molar Al/S ratios for basaluminite dissolution experiments conducted in  $\text{H}_2\text{SO}_4$  and  $\text{HCl}$  solutions at  $T = 291\text{-}295\text{ K}$  (data from Table 1).



## SUPPLEMENTARY INFORMATION

**Figure S1.** XRD of initial synthetic basaluminite sample. D-spacings and hkl assignments based on Farkas and Pertlik<sup>1</sup>.

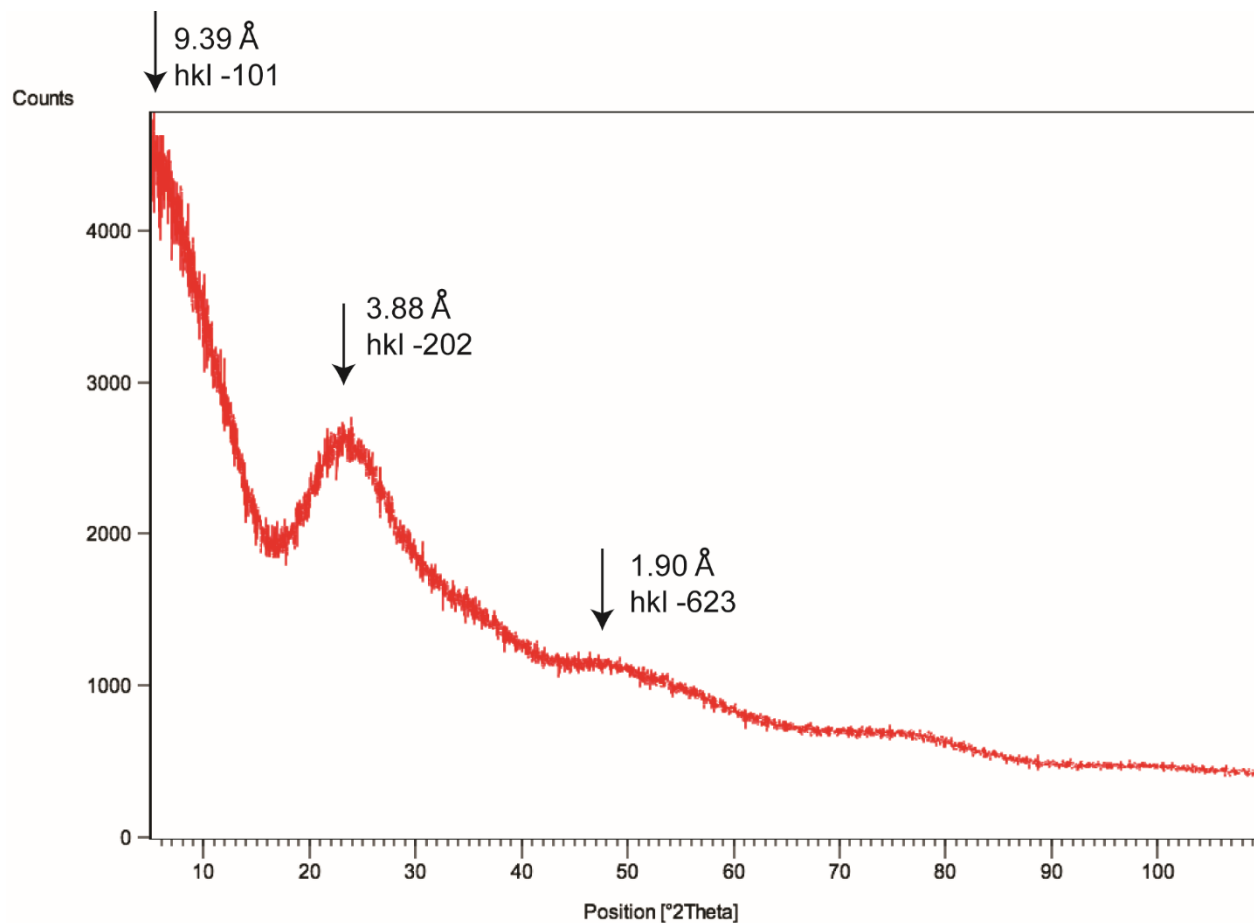




**Table S1.** Saturation indices in the final solutions from the different experimental conditions explored in this study with respect to the main possible aluminum secondary phases, calculated for the end of the experiments. Positive values correspond to theoretical oversaturation (precipitation thermodynamically favoured) and negative values indicate theoretical oversaturation (precipitation thermodynamically hindered). For the calculations, the largest concentrations achieved in any of the replicate experiments for each set of conditions have been selected.

pH	Solution type	T (K)	Al(OH) <sub>3</sub> (a)	Basaluminite	Diaspore (AlOOH)	Gibbsite (Al(OH) <sub>3</sub> )	Jurbanite (AlSO <sub>4</sub> (OH).5H <sub>2</sub> O)	Boehmite (AlOOH)
3.0	H <sub>2</sub> SO <sub>4</sub>	279	-7.43	-13.43	-3.42	-4.56	-1.58	-5.30
3.1	H <sub>2</sub> SO <sub>4</sub>	293	-6.66	-13.89	-2.71	-3.91	-1.67	-4.47
3.0	H <sub>2</sub> SO <sub>4</sub>	303	-5.53	-12.38	-1.63	-2.88	-1.31	-3.29
3.1	H <sub>2</sub> SO <sub>4</sub>	312	-4.43	-10.52	-0.57	-1.87	-0.92	-2.15
2.4	H <sub>2</sub> SO <sub>4</sub>	291	-8.43	-19.23	-4.48	-5.68	-1.72	-6.24
3.5	H <sub>2</sub> SO <sub>4</sub>	292	-5.21	-9.52	-1.26	-2.46	-1.65	-3.02
4.1	H <sub>2</sub> SO <sub>4</sub>	292	-3.75	-5.25	0.20	-1.00	-1.77	-1.56
3.6	HCl	294	-4.85	-9.66	-0.91	-2.12	-2.38	-2.65
4.0	HCl	293	-3.58	-5.07	0.37	-0.84	-1.80	-1.38
2.9	HCl	295	-6.42	-14.76	-2.48	-3.70	-2.66	-4.22
2.4	HCl	294	-8.25	-21.13	-4.31	-5.52	-3.65	-6.05

## REFERENCES

(1) Farkas, L., Pertlik, F. Crystal structure determinations of felsöbányaite and basaluminite,

$\text{Al}_4(\text{SO}_4)(\text{OH})_{10}\cdot 4\text{H}_2\text{O}$ . *Acta Mineral. Petrog. Szeged.* **1997**, 38, 5-15.